Supplement of

Temporal changes in rainfall intensity-duration thresholds for post-wildfire flash floods and sensitivity to spatiotemporal distributions of rainfall

Tao Liu et al.

Correspondence to: Tao Liu (liutao@arizona.edu)

S1: Examples of the four general spatial patterns of high intensity precipitation observed in upper Arroyo Seco watershed and around the region of interest

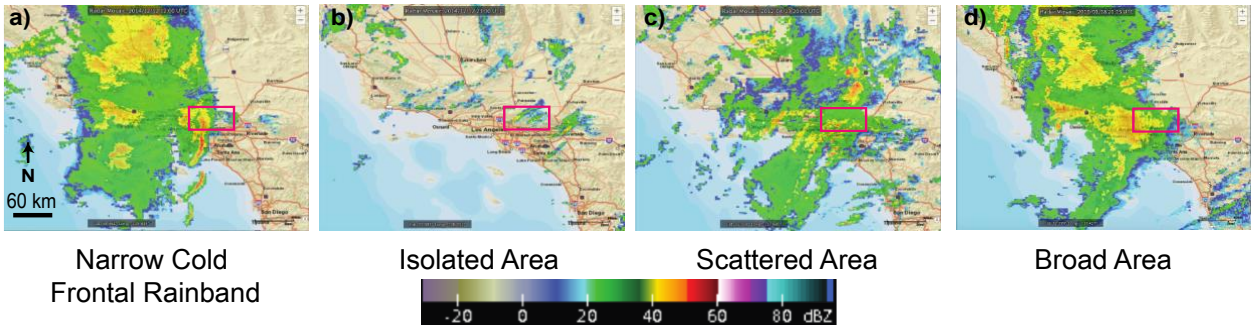

Figure S1: Examples of the four general spatial patterns of high intensity precipitation observed in this study in and around the region of interest as described in Section 3.1. Color fill represents composite radar reflectivity (dBZ) and the red box indicates the general location of the Station Fire burn area. Images sourced from the National Centers for Environmental Information Radar Data Map (https://gis.ncdc.noaa.gov/maps/ncei/radar).

S2: List of 34 storm events utilized in this analysis.

Table S1: List of 34 storm events utilized in this analysis are grouped by the spatial precipitation pattern type. Dates are given in format month/day/year. The first column assigns a number to the event. The second column provides the calendar date (represented as "Local Standard Time", or "LST") on which the event occurred. The third and fourth column provide the radar start date/time and end date/time, respectively, for which radar data were acquired for the event in UTC time. The fifth column provide the event moved over the San Gabriel Mt. The methods for defining start and end times are described in section 3.1.

	Event date (LST)	RADAR Start time (UTC)	RADAR End time (UTC)	Storm Event time (UTC)
NCFR				
1	12/29/2004	12/29/2004 1:00	12/30/2004 0:00	08:00-09:00
2	1/2/2006	1/2/2006 11:00	1/3/2006 4:00	17:00-20:00
3	3/17/2012	3/17/2012 9:00	3/17/2012 23:00	17:00-18:00
4	2/28/2014 (#1)	2/28/2014 10:00	2/28/2014 20:00	16:00-18:00
5	2/28/2014 (#2)	2/28/2014 21:00	2/29/14 15:00	23:00-23:59
6	12/12/2014	12/12/2014 9:00	12/12/2014 21:00	13:00-13:59
7	3/11/2016	3/11/2016 21:00	3/12/2016 1:00	23:00-23:59
8	2/17/2017	2/17/2017 21:00	2/18/2017 6:00	23:00-02:00
9	12/31/2004	12/31/2004 13:00	12/31/2004 20:00	18:00-18:59
10	3/20/2011	3/20/2011 16:00	3/21/2011 7:00	04:00-04:59
11	3/25/2012	3/25/2012 20:00	3/26/2012 1:00	23:00-23:59
12	1/9/2018	1/9/2018 7:00	1/9/2018 19:00	14:20-14:59
Isolated				
13	11/13/2009	11/13/2009 6:00	11/13/2009 11:00	06:28-06:59
14	12/13/2014	12/12/2014 22:00	12/13/2014 3:00	00:00-00:59
15	7/19/2015	7/20/2015 0:00	7/20/2015 6:00	02:00-02:59
16	10/11/2012	10/11/2012 17:00	10/12/2012 2:00	19:00-19:59
17	12/22/2010	12/22/2010 15:00	12/23/2010 3:00	19:00-20:00
Broad				
18	12/16/2002	12/16/2002 20:00	12/17/2002 3:00	00:00-00:59
19	3/15/2003	3/15/2003 17:00	3/16/2003 2:00	00:00-00:59
20	10/27/2004	10/27/2004 0:00	10/27/2004 13:00	05:00-05:59
21	12/19/2010	12/19/2010 14:00	12/20/2010 5:00	22:00-22:59
22	12/21/2010	12/20/2010 19:00	12/21/2010 6:00	02:00-02:59
23	1/4/2008 to 1/5/2008	1/5/2008 0:00	1/5/2008 14:00	06:00-09:00
24	10/20/2004	10/20/2004 0:00	10/20/2004 17:00	04:00-10:00
25	1/18/2010	1/18/2010 17:00	1/19/2010 2:00	20:00-20:59
26	2/16/2009	2/16/2009 15:00	2/16/2009 23:59	17:00-17:59
Scattered				
27	2/27/2010	2/27/2010 10:00	2/27/2010 20:00	15:15-15:59
28	4/13/2012	4/13/2012 17:00	4/13/2012 23:59	20:00-20:59

29	12/28/2004	12/28/2004 2:00	12/28/2004 22:00	18:00-18:59
30	12/29/2004	12/29/2004 1:00	12/29/2004 23:59	04:00-04:59
31	11/29/2018	11/29/2018 10:00	11/29/2018 20:00	16:00-16:59
32	1/17/2019	1/17/2019 2:00	1/17/2019 23:00	16:00-17:00
33	1/5/2016	1/5/2016 16:00	1/5/2016 23:59	22:00-22:59
34	1/6/2016	1/6/2016 17:00	1/7/2016 3:00	21:00-21:59

S3: Description of Z-R relationships applied to radar reflectivity observations in this study

As described in Section 3.1 of the text, five Z-R relationships were applied in this study. The purpose of this is twofold: first, no ideal Z-R relation exists for the western US and the high-intensity, often convective, rainfall events of interest to the post-fire flash flood problem. Applying the five Z-R relations provides a range of potential precipitation estimates. Second, we are using the KINEROS2 model to infer rainfall thresholds for post-wildfire flash floods. Thus, it is valuable to utilize five realizations of precipitation values for each storm event to span a broad range of precipitation intensities within each event and across events.

The five Z-R relationships applied and associated justifications are as follows:
1. **WSR-88** ($Z=300R^{1.4}$): This is the standard convective Z-R relationship used operationally by the National Weather Service (e.g., Nelson et al. 2009). It is also used as the relation applied to non-tropical convection by the operational Multi-Radar, Multi-Sensor (MRMS) product algorithm (Zhang et al. 2016).
2. **Marshall-Palmer (**$Z=200R^{1.6}$): This relation is derived from winter stratiform rain in southeast Canada. It is used as relation for cool stratiform rain when Z>40 dBZ by the operational MRMS algorithm and used operationally by NWS for stratiform precipitation (Nelson et al. 2009; Martner et al. 2005).
3. **Ron Brown** ($Z=466R^{1.47}$): Derived from disdrometer on the NOAA Ron Brown vessel during a field campaign involving a convective atmospheric river (Norris et al. 2020).
4. **Matrosov**: ($Z=75R^{2.0}$): This relation was derived from disdrometer and other meteorological observations during atmospheric river events in northern CA (near Cazadero). This study examined several Z-R relations and this one was found to perform best for atmospheric river events. (Matrosov et al. 2014).
5. **Martner Bright Band** ($Z=168R^{1.58}$): This threshold was developed for northern CA storms for both bright band and non-bright band precipitation (Martner et al. 2008). We utilize the the bright band relation here as we are not likely to be in a scenario dominated by warm rain processes (which are typically associated with non-bright band precipitation).

S4: Spatial distributions of the peak intensities for a storm result from the application of the five different Z-R relationships

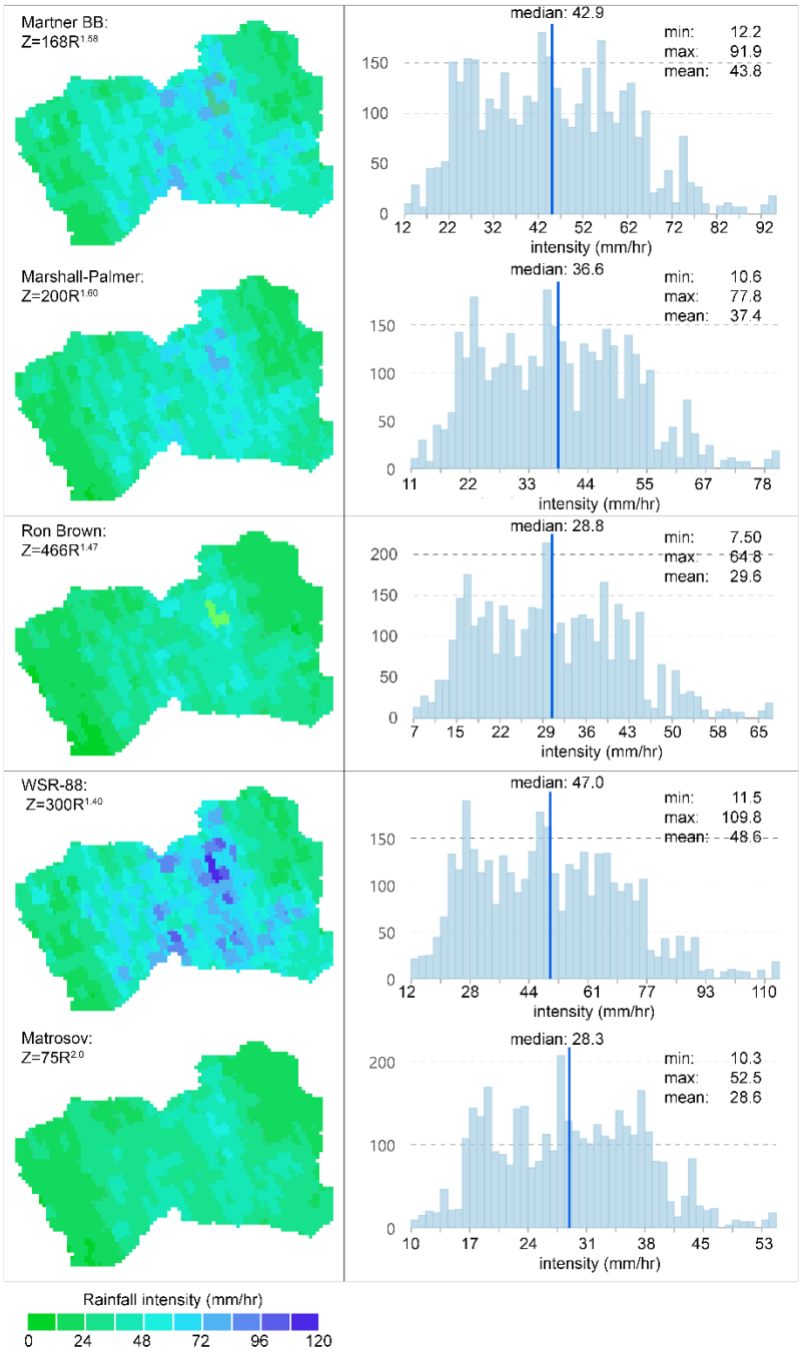

Figure S2: Spatial distributions of the peak intensity of the storm in Dec 22, 2010 resulting from the application of different Z-R relations

S5: Flood Frequency analysis at the outlet of the study watershed

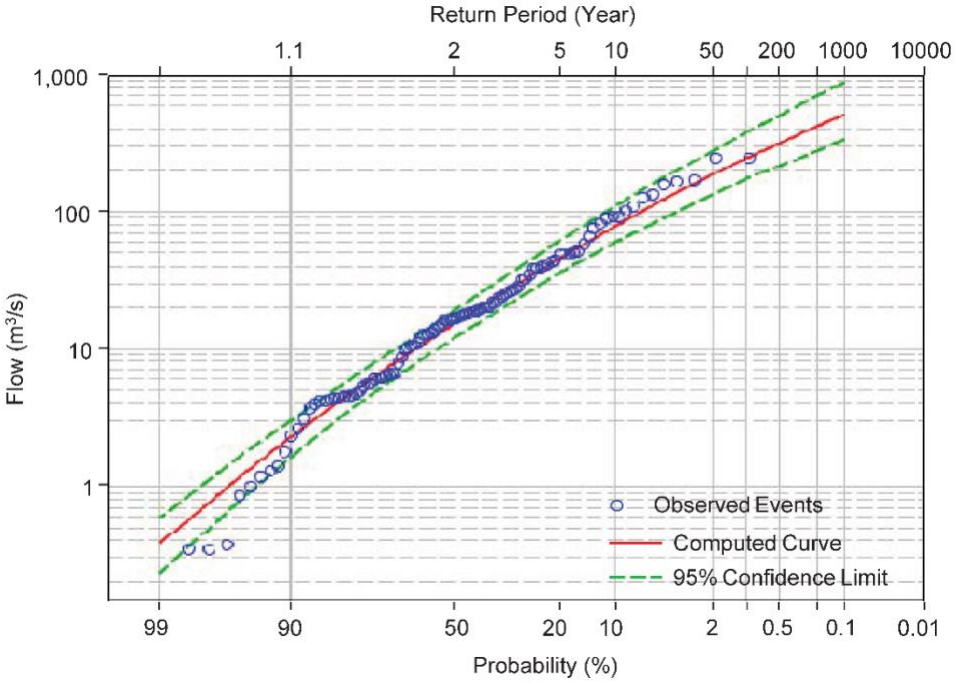

Figure S3: Results of flood frequency analysis (FFA) using annual peak flows (1914-2019) at U.S. Geological Society stream gage (11098000) on the upper Arroyo Seco watershed.

References:

Martner, B. E., Yuter, S. E., White, A. B., Kingsmill, D. E., & Ralph, F. M. (2005, October). Raindrop size distribution and Z–R relations in coastal rainfall for periods with and without a radar brightband. In *AMS 11th conference on mesoscale processes, Albuquerque, NM*.

Matrosov, S. Y., Ralph, F. M., Neiman, P. J., & White, A. B. (2014). Quantitative assessment of operational weather radar rainfall estimates over California's Northern Sonoma County using HMT-West data. *Journal of Hydrometeorology*, *15*(1), 393-410.

Nelson, B. R., Seo, D. J., & Kim, D. (2010). Multisensor precipitation reanalysis. *Journal of Hydrometeorology*, *11*(3), 666-682.

Norris, J. R., and Coauthors, The Observed Water Vapor Budget in an Atmospheric River over the Northeast Pacific. *J. Hydrometeor.*, doi: https://doi.org/10.1175/JHM-D-20-0048.1.

Zhang, J., Howard, K., Langston, C., Kaney, B., Qi, Y., Tang, L., ... & Arthur, A. (2016). Multi-Radar Multi-Sensor (MRMS) quantitative precipitation estimation: Initial operating capabilities. *Bulletin of the American Meteorological Society*, *97*(4), 621-638.